Chapter 3

SAMPLING AND ANALYTICAL METHODS

3.1 Pyrrhotite sampling

Pyrrhotite samples have been sourced from a variety of magmatic sulfide deposits in order to satisfy several criteria. The first of which is that the pyrrhotite deposits are of some economic relevance either due to the presence of the nickel hosted in pentlandite or due to the presence of the platinum group elements and platinum group minerals in these ore deposits. It was also desirable to obtain pyrrhotite samples where solely magnetic, solely non-magnetic and mixtures of magnetic and non-magnetic pyrrhotite were present. The capability to produce high grade pyrrhotite samples for mineral reactivity and microflotation tests was also a criteria in the selection of pyrrhotite samples for study.

3.1.1 Merensky Reef

Pyrrhotite samples were sourced from the Merensky Reef located at Impala Platinum Mines, near Rustenburg, South Africa. Two samples were used, namely samples *IMP-1* as shown in figure 3.1 and sample *IMP-2*, both of which represented cross sections through the basal portions of the Merensky Reef.

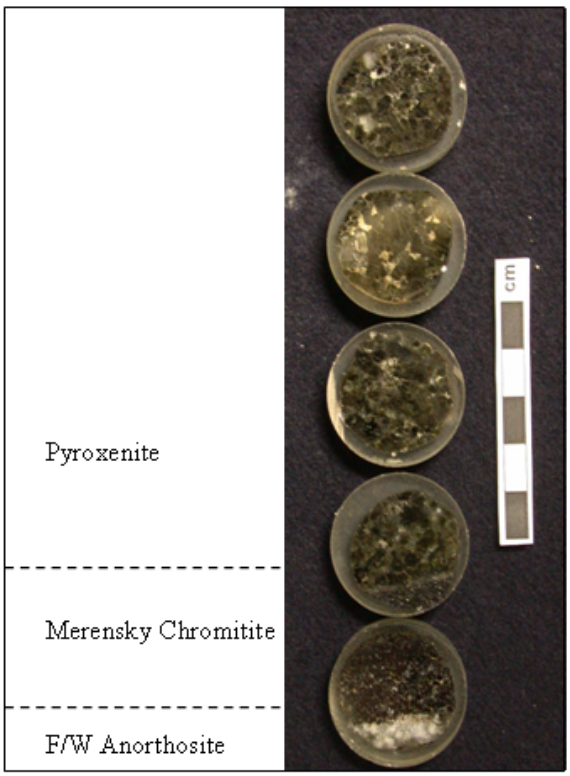

Figure 3.1: Photograph of the ore mounts from the Merensky Reef sample *IMP-1* used for pyrrhotite characterisation. F/W refers to the footwall.

3.1.2 Nkomati

Pyrrhotite samples were sourced from the Nkomati Nickel mine, Uitkomst Complex, near Barberton in South Africa from the massive sulfide body (MSB) and main mineralized zone (MMZ) of the mine by Nkomati personnel. Samples were extracted from the mine in January 2008 and the same sample batch was used for pyrrhotite characterisation, mineral reactivity and microflotation test work. Hand specimens of the samples used are shown in figure 3.2a, b.

3.1.3 Phoenix

Pyrrhotite samples were sourced from the Phoenix ore body at Tati Nickel mine near Francistown, Botswana. Massive sulfide samples occurring as veins in the host rock were accordingly hand picked from the Phoenix open pit. Samples were extracted from the mine in 2005 and the same sample batch was used for pyrrhotite characterisation, microflotation and

Figure 3.2: Photographs of the pyrrhotite samples used from (a) Nkomati MSB, (b) Nkomati MMZ (sample *MMZ-1*), (c) Phoenix, (d) Sudbury CCN, (e) Sudbury Gertrude and (f) Sudbury Gertrude West. The scale bars shown represent 5cm. Field of view for (d) and (e) is ~ 30cm. Photographs (d) and (e) courtesy of Vale INCO.

mineral reactivity test work. A photograph of a hand specimen representative of the Phoenix pyrrhotite used is shown in figure 3.2c.

3.1.4 Sudbury Copper Cliff North

Pyrrhotite samples were sourced from the Copper Cliff North mine, Sudbury Igneous Complex in Ontario, Canada by VALE Inco personnel from level 2400 of the 100 ore body at Copper Cliff North. Pyrrhotite from the 100 ore body is known to be unique in that it tends to be more than 90% non-magnetic whereas for the other ore bodies, the magnetic phase dominates (A. Kerr, Pers. Comm., 2007). Samples for pyrrhotite characterisation and microflotation tests were sourced from the mine in 2006 (Figure 3.2d), whereas the sample used for oxygen uptake tests was sourced from the mine in 2008. The sulfide grade for both samples was similar although the latter sample tended to be slightly more chalcopyrite rich.

3.1.5 Sudbury Gertrude and Gertrude West

Pyrrhotite samples for characterisation from the Gertrude mine, Sudbury Igneous Complex in Ontario, Canada were sourced by VALE Inco personnel from the Gertrude open pit mine in 2006. These samples were used for pyrrhotite characterisation and microflotation tests (Figure 3.2e). Since very poor recovery was obtained in microflotation tests for the original Gertrude pyrrhotite sample, a new sample was sourced in 2008 (Figure 3.2f). The new sample however, was derived from the Gertrude West ore body located 200 m west of the Gertrude mine. Initial mineral characterisation of the Gertrude West sample showed its mineralogical similarity to the original Gertrude sample in terms of petrography and mineral chemistry, and so the Gertrude West sample was then used in subsequent mineral reactivity and microflotation tests.

3.2 Mineralogical Characterisation

3.2.1 Optical Microscopy

Petrography of pyrrhotite samples was performed using a standard Zeiss petrographic microscope. Determination of magnetic and non-magnetic phases was performed with the use of a magnetic colloid (see associated photomicrographs in Section 4.2). The colloid was prepared by making a mixture of $FeCl_2$ and $FeCl_3$ particles to create an insoluble black magnetite precipitate which was stored in a soapy solution of sodium oleate as described by Craig and Vaughan (1981). Droplets of wet colloid were placed over the surface of the ore mount, the magnetic particles given a few seconds to interact with the pyrrhotite before the sample was viewed under the microscope and the image captured using a digital camera before the colloid dried on the sample. After use the colloid was wiped off the ore mount. Intergrowth textures and patterns highlighted by the colloid were observed to be the same for any particular sample when repeated immediately, or even several months later.

3.2.2 Powder X-ray Diffraction

Powder X-ray diffraction was used for the routine determination of mineralogy in ore samples on a Panalytical X'Pert Pro diffractometer with XCelerator detector housed at the University of Pretoria. Samples were run with automatic divergence slits using cobalt Kα radiation as the x-ray source. Samples were run from 5 to 90^0 2θ using a step size of 0.001^0. Samples run in order to confirm the crystallography were prepared by hand picking pyrrhotite grains from a crushed sample and mounted on a low background plate. Samples prepared for phase quantification, were taken from the microfloat feed sample or oxygen uptake sample, and subsampled with a Fritsch rotary sample divider. These samples were further subsampled using a Quantachrome microriffler. The final aliquot was micronized in ethanol using a McCrone micronizer. Phase quantification was carried out using the BGMN Autoquan Rietveld refinement software.

Phase quantification with the Autoquan Rietveld software was used to determine the proportion of sulfides for both oxygen uptake and microflotation feed samples so that

Table 3.1: Summary table of the mineralogy of samples used in oxygen uptake and microflotation tests. The proportion of pyrrhotite (po), pentlandite (pent), chalcopyrite (ccp), pyrite (py) as well as the total amount of base metal sulfides (BMS) and other minerals (mostly silicates) is also given in wt % as determined by QXRD using the Autoquan software. The associated 2σ standard deviation of the Rietveld refinement is also shown. Samples used for MLA characterisation are also distinguished.

Sample Details	**Phoenix** Mag Po		**Nkomati** Mixed Po		**Sudbury CCN** Non-mag Po		**Sudbury Gertrude** Mag Po		**Sudbury Gertrude West** Mag Po	
Test	O_2	Float	O_2	Float	O_2	Float	O_2	Float	O_2	Float
MLA	X	-	X	X	-	X	-	-	X	X
Po	-	88.6	85.9	85.9	62.1	68.7	-	63.0	86.8	86.8
2σ	-	*(0.24)*	*(0.32)*	*(0.32)*	*(1.18)*	*(2.00)*	-	*(0.66)*	*(1.58)*	*(1.58)*
Pent	-	11.3	6.27	6.27	6.12	6.88	-	5.48	9.53	9.53
2σ	-	*(0.24)*	*(0.20)*	*(0.20)*	*(0.30)*	*(0.34)*	-	*(0.11)*	*(0.28)*	*(0.28)*
Ccp	-	0.13	-	-	3.50	-	-	-	-	-
2σ	-	*(0.13)*	-	-	*(0.16)*	-	-	-	-	-
Pyrite	-	-	-	-	-	-	-	1.12	-	-
2σ	-	-	-	-	-	-	-	*(0.13)*	-	-
Other	-	0.00	6.86	6.86	28.3	11.4	-	30.4	4.77	4.77
BMS	-	*100*	*92.2*	*92.2*	*71.7*	*75.6*	-	*69.6*	*96.3*	*96.3*

collector and activator dosages could be accordingly calculated based on the total amount of base metal sulfides in the feed sample as shown in table 3.1.

3.2.3 Single Crystal X-ray Diffraction

Single crystal x-ray diffraction was used in order to determine unit cell dimensions of pyrrhotite crystals. Pyrrhotite single crystals from Sudbury CCN and the Impala Merensky (sample *IMP-1*) were measured on the diffractometer at the University of Pretoria whereas the Phoenix pyrrhotite sample was run on the diffractometer at the University of Cape Town. It was not possible to obtain single crystals suitable for x-ray diffraction for the remaining pyrrhotite localities.

The Phoenix pyrrhotite single crystal was mounted on a nylon loop suspended in oil and run on a Nonius Kappa CCD instrument at the University of Cape Town. The diffractometer was run at 50kV and 30mA for x-ray generation to produce monochromated molybdenum Kα

radiation with a graphite crystal monochromator. The analysis of pyrrhotite was performed at room temperature.

The Sudbury CCN and Impala Merensky (sample *IMP-1*) pyrrhotite single crystals were mounted on a glass fibre and run on a Siemens P4 diffractometer with Bruker SMART 1K CCD detector at the University of Pretoria. The diffractometer was run at 50kV and 30mA for X-ray generation to produce monochromated molybdenum Kα radiation with a graphite crystal monochromator. The analysis of pyrrhotite was performed at room temperature.

3.2.4 Electron Microprobe Analysis

Pyrrhotite compositions were analysed from several polished ore mounts derived from each locality on a Jeol JXA 8100 Superprobe housed at the Department of Geological Sciences, University of Cape Town. Pyrrhotite samples were analysed using an accelerating voltage of 25 kV and probe current of 20 nA. Iron and sulfur standardisation was performed on a meteoritic troilite standard from the Smithsonian Institution whereas nickel, copper and cobalt were calibrated against pure metal standards. Counting times for peak and background were 10 and 5 seconds, respectively. The relative instrument detection limits and standard deviations for measurements are given in table 3.2. A synthetic troilite specimen was also made by fusion of analytical grade iron and sulfur in an evacuated silica glass tube. The sample was placed in a furnace for 2 days at 400^0C and then a further 2 days at 800^0C prior to cooling, upon which the silica tube was manually fractured and the resulting troilite prepared into an ore mount for optical microscopy and microprobe calibration verification. The prepared ratio of Fe/S in the silica glass tube was such that the system was suitably iron saturated to ensure no non-stoichiometry or formation of pyrrhotite. This is reflected in the optical photomicrograph shown in figure 3.3 which displays zones of native iron indicating the reducing environment during troilite formation. The measured atomic iron / sulfur ratio of the synthetic troilite was 0.996 ± 0.01 (2σ) ensuring that the calibration procedure of the electron microprobe (EMP) based on the meteoritic troilite was suitable. The complete pyrrhotite mineral chemistry dataset is given in Appendix A1.

Table 3.2: Lower limit of detection (LLD) and 2-sigma standard deviation on pyrrhotite measurements using EMP operating conditions as described above.

Element	LLD (wt%)	2σ (wt%)
Ni	0.028	*(0.002)*
Cu	0.031	*(< 0.001)*
Co	0.032	*(< 0.001)*
Fe	0.041	*(0.118)*
S	0.032	*(0.108)*

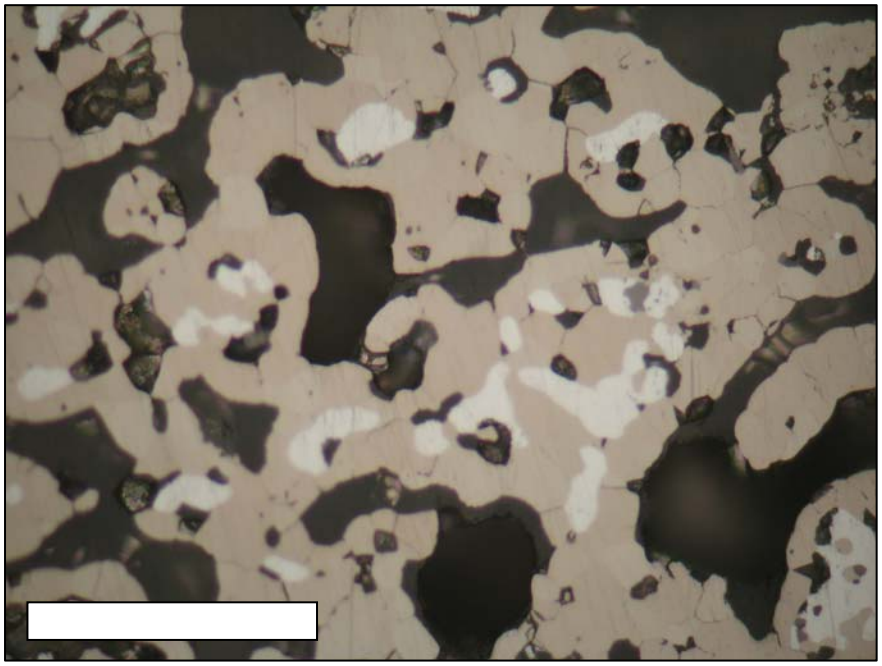

Figure 3.3: Reflected light photomicrograph of the synthetic troilite made for verification of the EMP standardisation. The pale cream phase is the troilite interrupted with occasional zones of bright white native iron. Scale bar represents 100 µm.

3.2.5 Automated SEM

Preliminary work in preparing a method for mapping magnetic and non-magnetic pyrrhotite was performed on a QEMSCAN® EVO50 located at Intellection, Brisbane in September 2006. Further developmental work in optimising the experimental routine was performed by Intellection in 2007 and the results of both sets of work are presented here (Section 3.3). Further details of the exact experimental conditions used can be found in Botha and Butcher (2008).

Mineralogical characterisation of microflotation feed samples by MLA was performed by Vale INCO Technical services in Sheridan Park, Toronto. The MLA consisted of a JEOL 6400 SEM fitted with two energy dispersive EDAX Si(Li) spectrometers with digital pulse processors. Measurements were run at 20 kV with counting times of 32 ms per pixel using the GXMAP routine in order to determine the relative proportion of all mineral phases present which are shown in table 3.3. All particles containing pentlandite, pyrrhotite, chalcopyrite and pyrite were individually mapped by the MLA. The liberation characteristics of pyrrhotite and pentlandite were also determined and are given in Appendix C1.

Table 3.3: Composition of pyrrhotite samples as determined by MLA and used for the experimental test work programme. See table 3.1 for specific details regarding samples used for oxygen uptake or microflotation tests.

Mineral (wt %)	**Phoenix** Magnetic Po	**Nkomati MSB** Mixed Po	**Sudbury CCN** Non-magnetic Po	**Sudbury Gert West** Magnetic Po
Pyrrhotite	81.8	83.8	75.4	85.2
Pentlandite	16.9	6.61	7.87	8.21
Chalcopyrite	0.22	2.92	0.66	0.21
Pyrite	0.54	0.86	0.00	0.30
Other Sulphides	0.00	0.01	0.00	0.00
Olivine	0.07	0.05	0.35	0.14
Orthopyroxene	0.00	0.00	0.40	0.54
Clinopyroxene	0.01	0.00	0.00	0.00
Amphibole	0.06	0.06	3.36	0.92
Talc	0.00	0.00	0.00	0.00
Serpentine	0.00	0.00	0.00	0.00
Chlorite	0.02	0.03	0.20	0.89
Biotite	0.01	0.01	1.61	0.58
Plagioclase	0.00	0.07	6.42	1.14
Quartz	0.03	0.01	2.27	0.74
Calcite	0.00	0.01	0.02	0.00
Magnetite	0.19	5.49	1.11	0.61
Other oxides	0.01	0.01	0.26	0.30
Other	0.09	0.07	0.04	0.18
Total BMS	*99.5*	*94.2*	*84.0*	*94.0*
Total	*100*	*100*	*100*	*100*

3.3 Development of methodology for discrimination of pyrrhotite types

The overall approach used in order to review the methods for quantitative pyrrhotite analysis was considered in two phases. The first of which was to ensure that the Rietveld method in conjunction with powder XRD was able to successfully quantify the proportions of magnetic and non-magnetic pyrrhotite in mixed pyrrhotite samples. The aim of the second phase was to develop a method and prescribed operating parameters for phase quantification of magnetic and non-magnetic pyrrhotite using an automated SEM (e.g. QEMSCAN, MLA). It should be noted that the advantages of utilising an automated SEM is that the relative proportions, as well as the textural relationships between pyrrhotite phases can be quantified.

3.3.1 Analysis of pyrrhotite types using QXRD

Based on the characterisation of the Phoenix and Sudbury CCN pyrrhotite as pure (< 5 % of a second coexisting pyrrhotite phase) magnetic and non-magnetic pyrrhotite end-members, respectively (see Chapter 4), these two pyrrhotite samples were selected for powder XRD analysis to review the capability of the Rietveld method in order to quantify the relative proportions of pyrrhotite in a mixed sample. Successful phase quantification in QXRD is based upon the input of reference crystal structural information which is similar in character (e.g. crystallographic superstructure, composition, natural versus synthetic, phase stability) to the sample being analysed. The C2/c 4C pyrrhotite crystal structure of Powell *et al.* (2004) was used as the reference structure for Phoenix pyrrhotite, and the 5C pyrrhotite crystal structure from De Villiers *et al.* (Submitted) was used as the reference for Sudbury CCN pyrrhotite. The reference crystal structure of the C2 4C structure from sample *IMP-1* was also used (De Villiers *et al*., In Prep.).

A calibration curve was made by mixing the Phoenix magnetic pyrrhotite and Sudbury CCN non-magnetic pyrrhotite in carefully weighed out proportions such that the sample contained 0, 30, 50, 70 and 100 % magnetic pyrrhotite, respectively. Phase quantification to determine the relative proportions of magnetic 4C and non-magnetic 5C pyrrhotite was not successfully achieved using the Autoquan software since the user is unable to specify which parameters are refined. However, successful quantification was achieved using the Topas software and the diffractogram from the refinement is shown in figure 3.4. The key elements to the

successful determination of the relative proportions of magnetic and non-magnetic pyrrhotite in a mixture of pyrrhotite types, was based on the simultaneous refinement of all the samples. It was also necessary to constrain the crystallite size and unit cell parameters of the different pyrrhotite phases to be equal to one another for all the samples analysed. The final calibration curve comparing the actual and calculated proportions of magnetic C2/c 4C and non-magnetic 5C pyrrhotite in the calibration curve is shown in figure 3.5 where it is evident that the refinement works well for mixtures of pyrrhotite types, but slightly underestimates the proportion of pure magnetic C2/c 4C pyrrhotite.

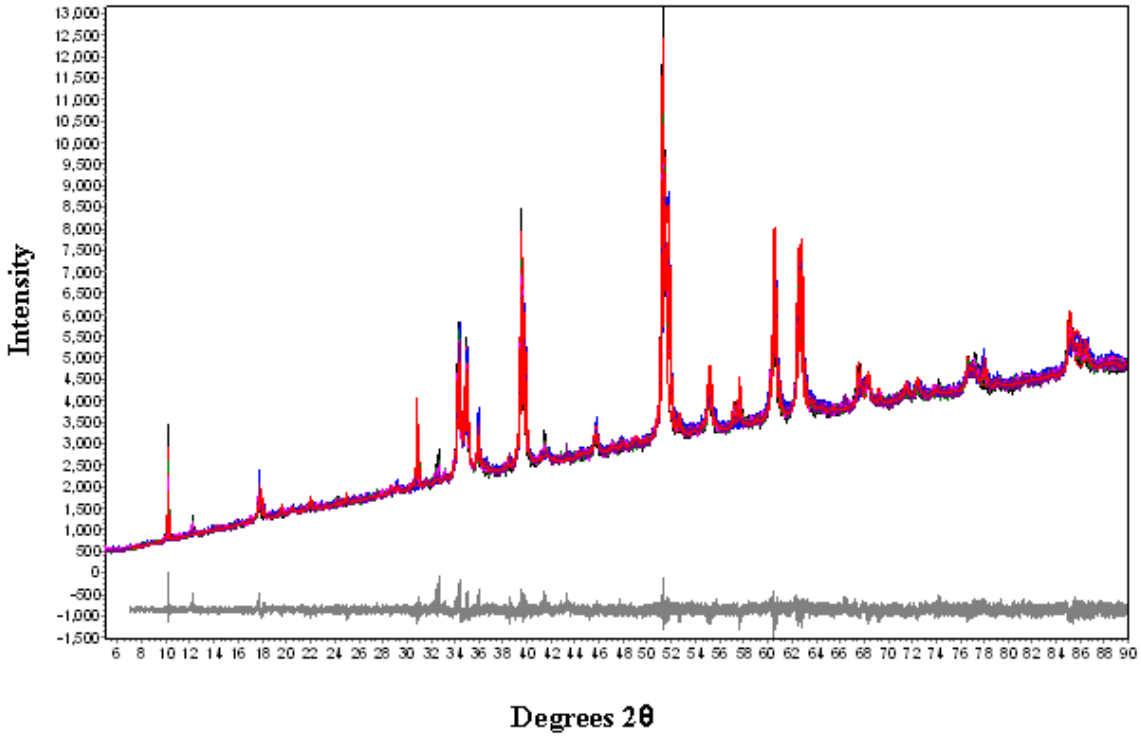

Figure 3.4: Diffractogram showing the results of the simultaneous Rietveld refinement of all the samples in the pyrrhotite calibration curve using Topas. The red line represents the calculated diffractogram, blue line represents the measured diffractogram and the grey line indicates the residual.

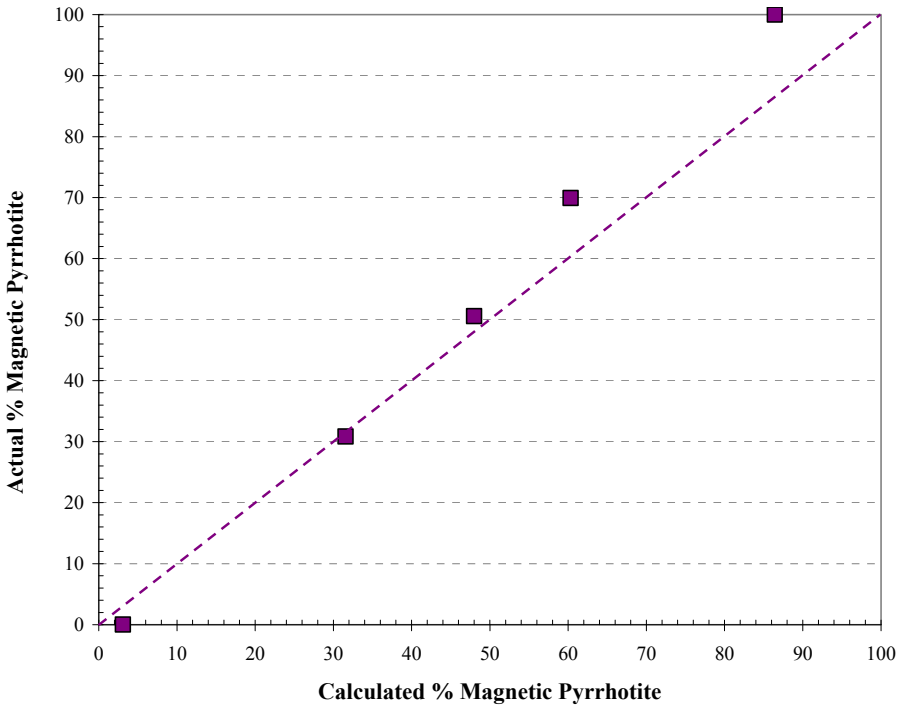

Figure 3.5: The calibration curve obtained for pyrrhotite phase quantification using the Topas Rietveld QXRD software. The proportion of magnetic *C2/c* 4C pyrrhotite is shown.

3.3.2 Analysis of pyrrhotite types using QEMSCAN

Nkomati MSB mixed pyrrhotite samples were initially viewed using only the BSE functionality of QEMSCAN under routine operating conditions in order to establish the relationship between magnetic and non-magnetic pyrrhotite. This test established two critical factors, the first of which was that the x-ray spectra of the different pyrrhotite phases captured by the energy dispersive detectors was unable to discriminate between the phases based entirely on composition. The second factor established was that the BSE grey level contrast between magnetic (~ 43.16) and non-magnetic pyrrhotite (~ 43.33) viewed using routine operating conditions was too subtle to reliably be used as a means to discriminate between pyrrhotite types (Figure 3.6 a, b), especially since it was subject to secondary effects such as polishing scratches. This prompted a series of developmental stages relating to the capture of the BSE signal by the QEMSCAN operating software and customised calibration settings of the QEMSCAN system in order to create a specialised routine for pyrrhotite mapping.

After numerous iterations and developments in brightness and contrast settings, as well as developments relating to the method in which the instrument obtained the BSE image were performed (Botha and Butcher, 2008), the QEMSCAN was able to successfully discriminate

between pyrrhotite types (Figure 3.6 c, d). Further work in order to perform a thorough data validation programme utilising optical microscopy, QXRD and EBSD in order to confirm the results shown in figure 3.6 is recommended before this is used as a standard procedure. It is however noted even with further validation and development of the QEMSCAN procedure, several limitations will still exist with this technology. This includes those features that affect the BSE signal, such as crystal orientation or anistropism and surface polishing (Section 2.2.8) as well as the likelihood of long measurement times to improve precision.

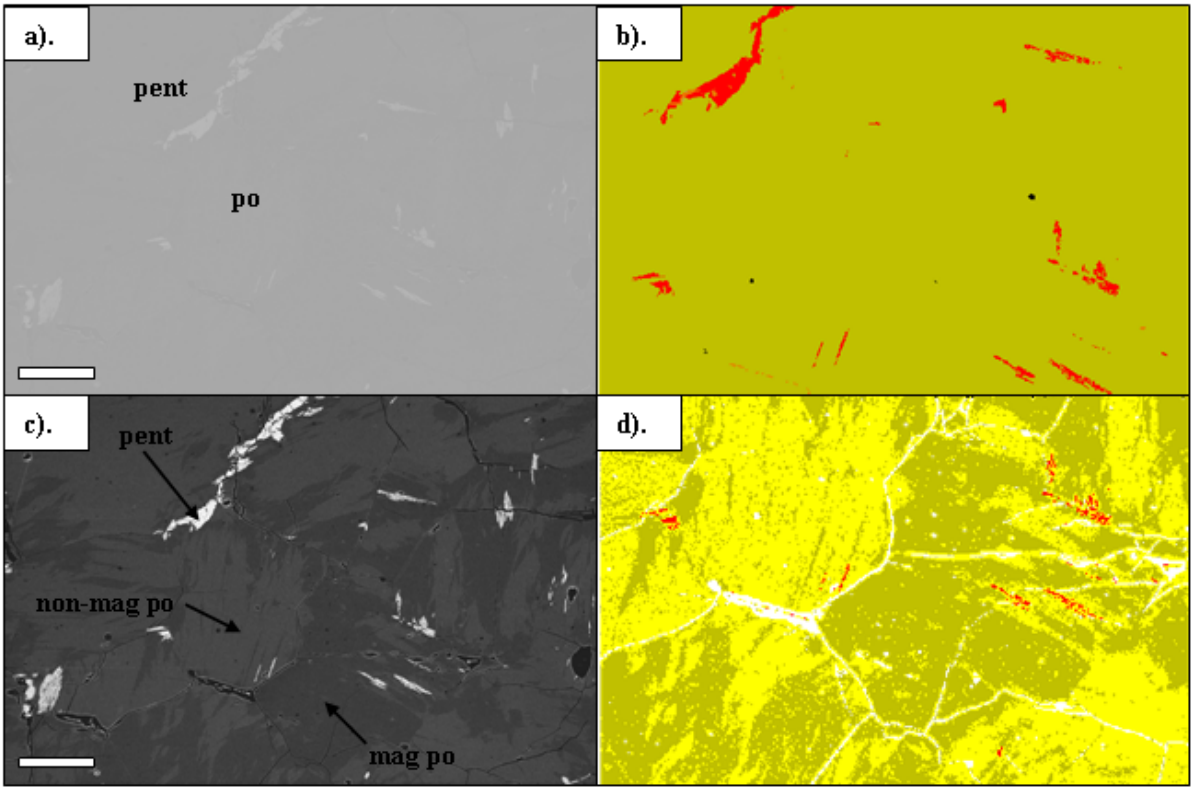

Figure 3.6: Summary of the BSE images (a, c) and the respective QEMSCAN false colour images (b, d) of Nkomati MSB pyrrhotite during the development of the pyrrhotite mapping technique. (a, b) show pyrrhotite under routine conditions whereas (c, d) show intergrown magnetic and non-magnetic pyrrhotite using adjusted SEM brightness and contrast settings in addition to specialised operating and calibration conditions. Colours used in the false colour QEMSCAN images are as follows: red – pentlandite, yellow – non-magnetic pyrrhotite, mustard – magnetic pyrrhotite. Scale bar represents 200 µm.

3.4 Pyrrhotite Reactivity

The reactivity of pyrrhotite samples was measured using a combination of both electrochemical measurements with pyrrhotite electrodes and determination of the oxygen uptake of pyrrhotite in mineral slurry. Both the open circuit potential and cyclic voltammetry measurements were performed at Haceteppe University in Turkey (Ekmekci *et al.*, Submitted), whereas oxygen uptake measurements were performed at the University of Cape Town.

3.4.1 Electrode Preparation

Working electrodes of the pyrrhotite samples in this study were manufactured by mounting a ~ 2 x 2 mm slice of pyrrhotite into an epoxy resin. Contact with the electrode was made by plating one side of the pyrrhotite surface with copper. A copper wire held in a glass casing was then attached to the copper plate. The electrodes were polished after every run with 500 grit SiC paper for 1 minute after which any residual particulate matter was removed in an ultrasonic bath. In order to confirm the purity of the mineral electrodes, BSE images and elemental maps of the electrodes were taken on an EVO 50 SEM with Bruker AXS XFlash 3001 Energy dispersive detectors at Hacettepe University. The annotated BSE images of the pyrrhotite working electrodes shown in figure 3.7 illustrate that the electrodes were slightly contaminated by minerals such as pentlandite, chalcopyrite, pyrite and magnetite. Figure 3.7 shows that pyrrhotite was however, always the dominant phase and since the focus of this study is on real ore samples, the electrodes were used as is.

3.4.2 Open Circuit Potential

Following preparation of the electrode as described in section 3.4.1, open circuit potential measurements were performed on the various pyrrhotite samples to determine the state of surface oxidation. An electrochemical cell containing the working electrode, reference electrode (calomel) and counter electrode (Pt wire) was set up in a 50 ml buffer solution. Open circuit potential measurements were performed at either pH 7 or 10 with buffer solution composition of 0.025M KH_2PO_4 + 0.025M Na_2HPO_4, or 0.025M $Na_2B_4O_7.10H_20$ + 0.1M

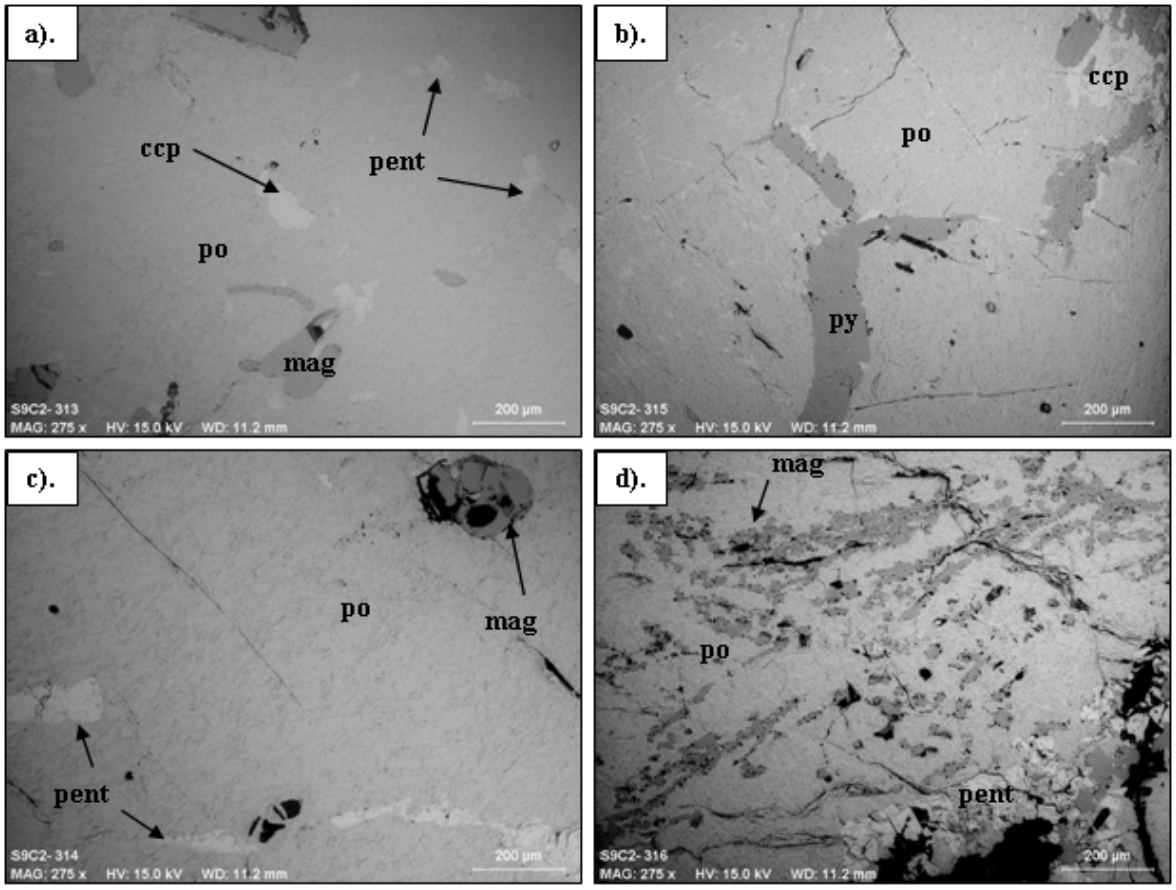

Figure 3.7: SEM BSE images of the pyrrhotite working electrodes used for electrochemical measurements. The contaminant minerals in the electrodes are shown. Images are shown for (a) Nkomati MSB mixed pyrrhotite (b) Phoenix magnetic pyrrhotite (c) Sudbury CCN non-magnetic pyrrhotite and (d) Sudbury Gertrude West magnetic pyrrhotite. Photograph courtesy of E. Bagci Tekes.

NaOH, respectively. Measurements were performed in deoxygenated solutions prepared by purging nitrogen gas through the solution prior to each experiment. Measurements were taken after 10 minutes to allow stabilisation of the potential. The solution was stirred continuously throughout the duration of the experiment. After each run, the surface of the electrode was repolished to prevent any poisoning of the electrode. Measurements were performed in triplicate. The raw data from open circuit potential measurements are presented in Appendix B1.

3.4.3. Cyclic Voltammetry

Cyclic voltammetry was used as an additional technique to compare the electrochemical characteristics of the different pyrrhotite samples examined in this study. The same electrode used in the open circuit potential measurements (Section 3.4.2) was used in the electrochemical cell illustrated in figure 3.8. The electrochemical cell was purged with nitrogen for 15 minutes at which point the clean electrode was transferred into the cell. Measurements were performed with a Gamry Instruments model PCl4/750 Potentiostat at a scanning rate of 20 mV per second. Scanning was initiated at open circuit potential and gradually taken to more negative potentials in order to remove any oxidised species formed on the electrode surface during polishing. The measured current was then converted to a current density based on the real surface area of the individual electrodes given in table 3.4, determined using a roughness factor of ~ 7. After each run, the surface of the electrode was repolished to prevent any poisoning of the electrode. All measurements were performed in duplicate. The complete set of cyclic voltammetry results is given in Appendix B2.

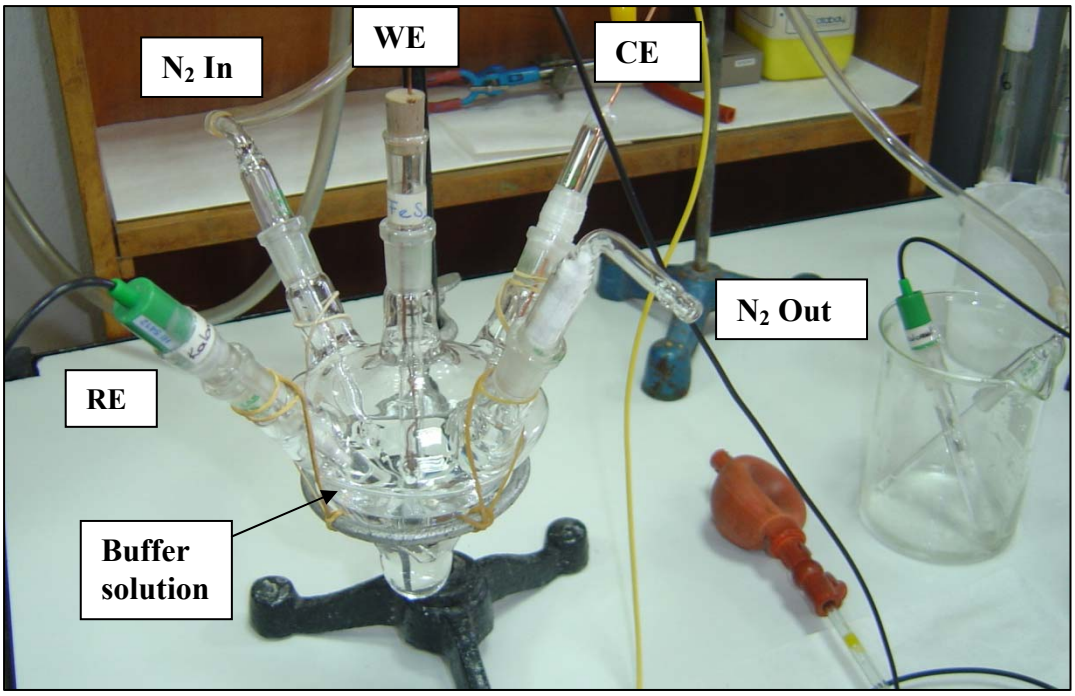

Figure 3.8: Photograph of the cell used for electrochemical measurements. The working pyrrhotite electrode (WE), reference electrode (RE) and counter electrode (CE) are annotated. Photograph courtesy of E. Bagci Tekes.

Table 3.4: Real surface area of the different pyrrhotite electrodes used for cyclic voltammetry.

Pyrrhotite	Mineralogy	Surface Area (cm2)
Nkomati MSB	Mixed	1.225
Phoenix	Magnetic	2.065
Sudbury CCN	Non-magnetic	1.505
Sudbury Gertrude West	Magnetic	1.750

3.4.4 Oxygen Uptake

An additional measurement used to compare the reactivity of different pyrrhotite samples was based on the rate of oxygen uptake of a pyrrhotite slurry through pyrrhotite oxidation. Using methodology developed by Afrox (Afrox, 2008), oxygen uptake factors were determined. The method is based upon the measurement of the rate of dissolved oxygen decay of a pyrrhotite slurry once the sample had been sparged with a controlled amount of pure oxygen. A schematic of the apparatus used for the oxygen uptake is illustrated in figure 3.9 and which consists of a dissolved oxygen probe connected to a TPS meter, in turn connected to a PDA computer.

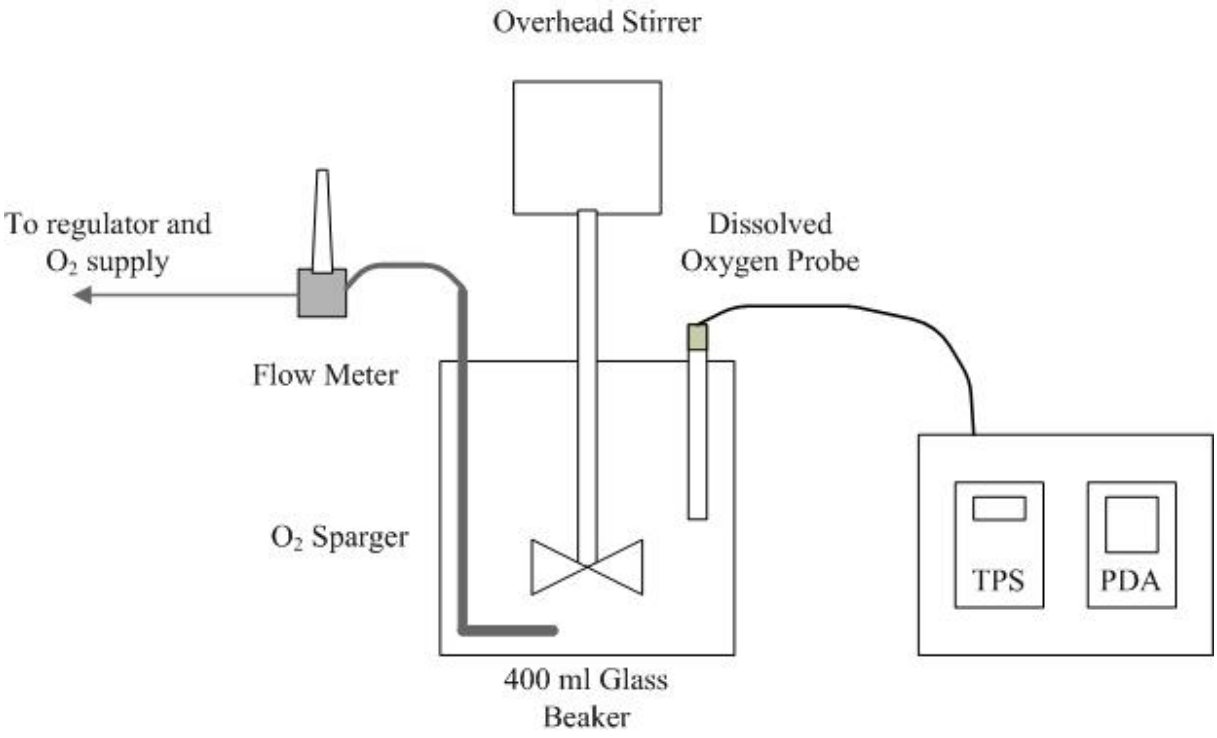

Figure 3.9: Diagram of the apparatus used for dissolved oxygen uptake measurements.

Pyrrhotite samples for oxygen uptake tests were prepared by crushing lumps of massive pyrrhotite with a jaw crusher and then dry milling with a Sieb mill. Samples were dry screened to the desired size fraction of 53 to 106 µm and then split and packaged into representative aliquots of ~ 80 g using a Fritsch rotary sample divider and stored in a freezer until needed. Where necessary, the pyrrhotite was upgraded by either hand picking out chips of silicate minerals from the jaw crush (Sudbury CCN), or removing excess chalcopyrite from the milled sample with a hand magnet (Sudbury CCN, Nkomati MSB).

At the start of the oxygen uptake tests, individual sample aliquots were ultrasonicated in distilled water to disaggregate any fine particles. The pyrrhotite was then wet screened at 53 µm with 3.33 x 10^{-3} M calcium water (10^{-2} ionic strength) and transferred into a 400 ml beaker for the oxygen uptake tests. Surface area measurements of pyrrhotite samples after ultrasonication were obtained using the Brunauer Emmet and Teller (BET) technique with nitrogen adsorption to check the equivalence of samples (Table 3.5). The pyrrhotite sample was made into a slurry using 300 ml of 3.33 x 10^{-3} M calcium water (10^{-2} ionic strength) at the desired pH to produce a slurry of ~ 25 % solids by weight. The mineral sample was then agitated with an overhead stirrer, dosed and conditioned with depressant, activator ($CuSO_4$) and collector respectively according to the specifications in table 3.6. Collector dosage was determined according to the proportion of BMS in the oxygen uptake sample as measured by QXRD and as shown in table 3.1. A collector dosage of 4.0 x 10^{-5} M was used for a sample containing ~ 100 % BMS (see Appendix B3). Activator dosage was based on a 0.4:1.0 ratio of copper to xanthate. This ratio was selected to ensure an excess of xanthate and minimise the formation of copper hydroxides. Collectors were supplied by SENMIN, Sty 504 guar from Chemquest and $CuSO_4.5H_2O$ from Merck. The sample was then modified to the desired pH with the use of NaOH or HNO_3 prior to the dissolved oxygen uptake measurements.

Table 3.5: BET surface area measurements of mineral samples used for oxygen uptake tests.

Pyrrhotite	Mineralogy	Surface Area ($m^2.g^{-1}$)
Phoenix	Magnetic	0.33
Sudbury CCN	Non-magnetic	0.22
Sudbury Gertrude West	Magnetic	0.32
Nkomati MSB	Mixed magnetic and non-magnetic	0.23

The dissolved oxygen content of the sample was then measured with a YSI 5739 DO probe fitted with YSI high speed membrane (1 s response) connected to a TPS WP-91 dissolved oxygen meter. Data from the TPS meter were extracted using a PDA computer. The pyrrhotite slurry was sparged with medical oxygen for 10 seconds at a flow rate of 1.15 $L.min^{-1}$ and controlled using a Sierra Smart Trak flow meter provided by Process Kinetics. Dissolved oxygen measurements were taken every 2 seconds for 2-3 minutes to measure the decay of the dissolved oxygen by the pyrrhotite slurry. The associated oxygen uptake factor was then calculated according to the methodology shown in Appendix B4. Due to considerable mass of pyrrhotite required in the correct size fraction for each test (~ 80 g in 53-106 µm) analyses were not performed in duplicate. Based on previous work by Becker *et al.* (2005) however, it is known that the repeatability is fair (see Appendix B4) and relative errors are ~ 10% on the calculated oxygen uptake factor. The complete set of oxygen uptake results is given in Appendix B5.

Table 3.6: Summary of the procedure used for oxygen uptake experiments.

Activity	Conditions	Time (min)
Retrieval of sample from freezer	~ 80g pyrrhotite sample (53-106 µm)	-
Ultrasonification	400 ml Distilled Water	5
Wet screening	Synthetic water @ desired pH, 10^{-2} ionic strength Ca^{2+}	-
Transferral into beaker	Sample stirring at point of depressant addition	-
Depressant addition	Sty 504 @ 10ppm	5
Activator addition*	$CuSO_4$ @ 1.6 X 10^{-4}M	2
Collector addition*	Xanthate (SIBX or SNPX) @ 4.0 X 10^{-4}M	2
pH modification	NaOH	-
DO measurement	-	-
O_2 Introduction	O_2 sparging at 1.15L.min^{-1}	10 sec
DO measurement	-	3

* Reagents are given for a sample containing 100% BMS.

3.5 Pyrrhotite Microflotation

3.5.1 Microflotation tests

Microflotation tests were conducted using the UCT microfloat cell illustrated in figure 3.10 and developed by Bradshaw and O' Connor (1996). The microfloat cell consists of a 365 ml columnar glass cell with launder. Synthetic air is injected into the base of the cell with a Hamilton syringe that produces a single bubble stream. Hydrophobic particles attached to these bubbles rise to the top of the cell where the bubbles burst when they hit a glass cone, and the hydrophobic particles fall into the launder to be collected as concentrates.

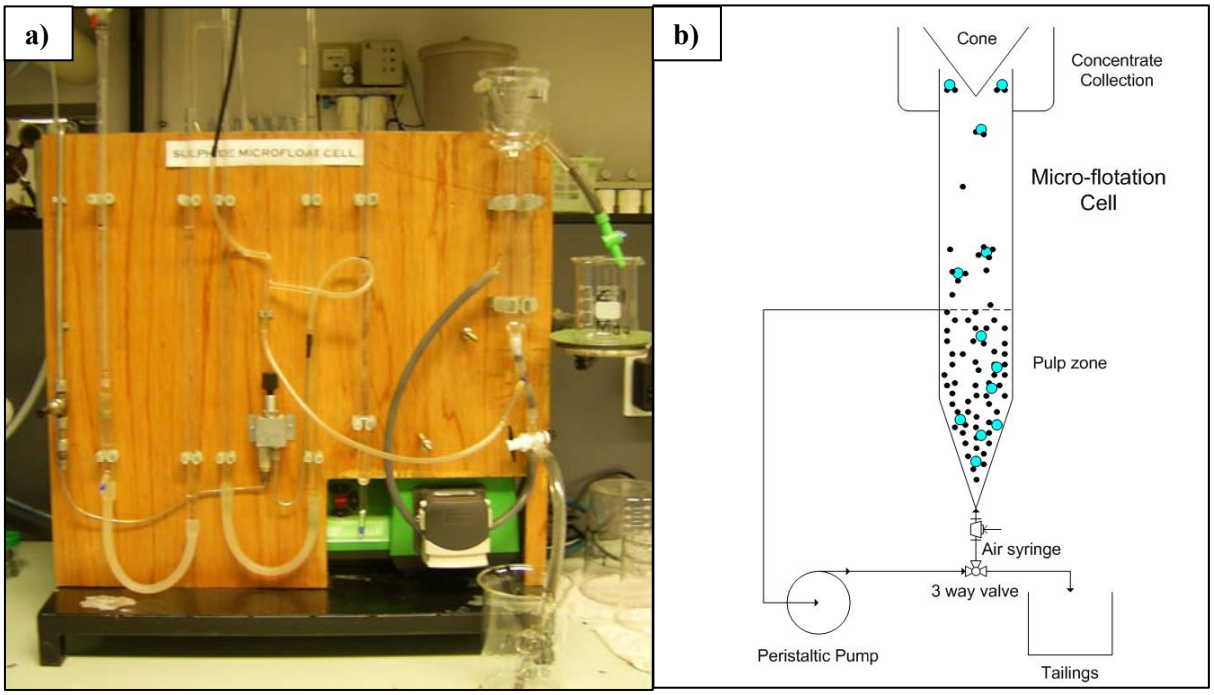

Figure 3.10: (a) Photograph and (b) diagram of the microflotation cell used for the tests in this study. From: Mbonambi (2009).

Microfloat tests were carried out using pyrrhotite which was prepared with a Sieb mill and then dry screened to the desired size fraction of 53 to 106 µm. Since the microflotation tests were only performed on high grade pyrrhotite samples, the Merensky Reef pyrrhotite samples were excluded from this set of test work. Pyrrhotite samples were stored in a freezer until needed for the microfloat test work programme. Surface area measurements of pyrrhotite samples prior to ultrasonication were obtained using the Brunauer Emmet and Teller

technique with nitrogen adsorption to check the equivalence of samples (Table 3.6). The morphology of the pyrrhotite microfloat samples was also examined using a Leica LEO Stereoscan S440 Scanning Electron Microscope at the University of Cape Town. Selected images of the pyrrhotite particles are shown in figure 3.11. Samples were examined both prior to and post ultrasonification to examine whether there were any significant differences in particle morphology of the pyrrhotite specimens examined.

Table 3.7: BET surface area measurements of mineral samples used for microflotation tests.

Pyrrhotite	Mineralogy	Surface Area ($m^2.g^{-1}$)
Phoenix	Magnetic	0.13
Sudbury CCN	Non-magnetic	0.23
Sudbury Gertrude	Magnetic	0.35
Sudbury Gertrude West	Magnetic	0.17
Nkomati MSB	Mixed magnetic and non-magnetic	0.13

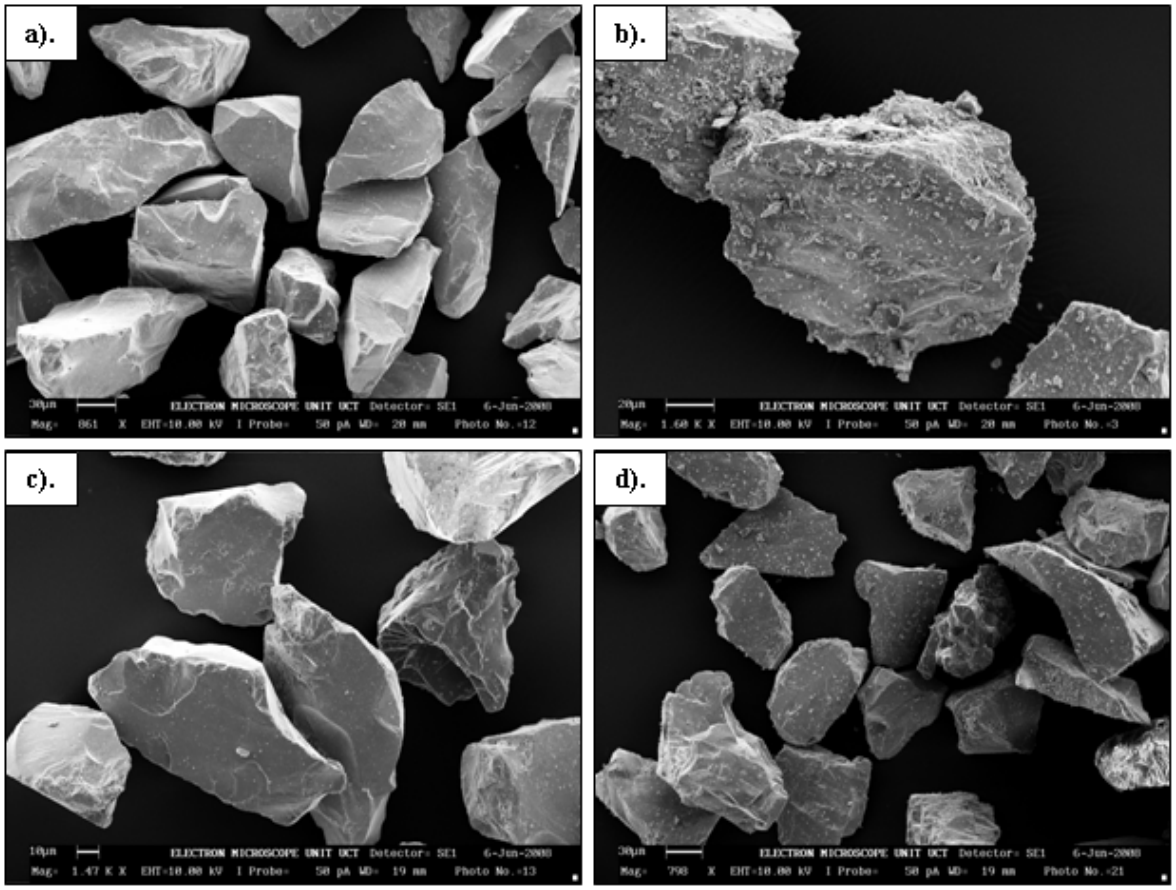

Figure 3.11: SEM images of ultrasonicated pyrrhotite particles used for microflotation tests. Images are shown for (a) Nkomati MSB mixed pyrrhotite, (b) Phoenix magnetic pyrrhotite, (c) Sudbury CCN non-magnetic pyrrhotite and (d) Sudbury Gertrude magnetic pyrrhotite.

2g of pyrrhotite was then carefully weighed out and ultrasonicated in distilled water for 5 minutes in order to detach fine material most likely derived from the oxidation of pyrrhotite. Following ultrasonification the sample was wet screened at 53 µm to remove the fines and transferred into the conditioning vessel with 3.33 x 10^{-3}M calcium water (10^{-2} ionic strength). The mineral sample was then agitated and dosed with depressant, activator (copper) and collector (SIBX, SNPX), respectively according to the specifications in Table 3.8. Collector dosage was determined according to the proportion of sulfide in the flotation feed sample as measured by QXRD (Table 3.1). Activator dosage was based on a 0.4:1.0 ratio of copper to xanthate. This ratio was selected to ensure an excess of xanthate and minimise the formation of copper hydroxides. Collectors were supplied by SENMIN, Sty 504 guar from Chemquest and $CuSO_4.5H_2O$ from Merck. The sample was then modified to the desired pH with the use of NaOH or HNO_3 and transferred into the microflotation cell. The exact reagent dosages used for each pyrrhotite sample are given in Appendix C2.

Table 3.8: Summary of the procedure used for microflotation tests.

Activity	Conditions	Time (min)
Sample weighing	2g pyrrhotite sample (53-106µm)	-
Ultrasonification	80 ml Distilled Water	5
Wet screening	Synthetic water @ desired pH, 10^{-2} ionic strength Ca^{2+}	-
Transferral into beaker	Sample stirring at point of depressant addition	-
Depressant addition	Sty 504 @ 10ppm	5
Activator addition*	$CuSO_4$ @ 0.4 X 10^{-5}M	2
Collector addition*	Xanthate (SIBX or SNPX) @ 1.0 X 10^{-5}M	2
pH modification	NaOH or HNO_3	-
Transferral into microfloat cell	100rpm pump speed, 7ml.min^{-1} synthetic air flow	-
Conc 1 Collection	-	2
Conc 2 Collection	-	3
Conc 3 Collection	-	5
Conc 4 Collection	-	5

* Reagent are given for a sample containing 100 % BMS

Flotation was initiated with the insertion of a Hamilton syringe needle into the base of the float cell at a flow rate of 7 ml.min^{-1} using synthetic air. The mineral sample was kept in

suspension by a peristaltic pump operating at 100 rpm. Mineral concentrates were collected after 2, 5, 10 and 15 minutes of flotation, carefully filtered and dried for further analysis. Recoveries were calculated either on the basis of total mass or calculated pyrrhotite from the chemical assay. All microflotation tests were conducted in duplicate. The complete set of flotation results is given in Appendix C3.

3.5.2 Analysis of Flotation Performance

Where sufficient pyrrhotite mass was available from the microflotation tests, samples were selected for chemical assay. Microflotation test concentrate and tails were measured for iron, nickel and copper using Atomic Absorption Spectroscopy (AA) and sulfur using a LECO Sulfur Analyser.

Samples for AA were prepared by the digestion of a carefully measured amount of pyrrhotite (between 0.05 and 0.1 g) in a mixture HF, HNO_3, $HClO_4$ and HCl using the acid digestion procedure as given in Brough (2008). Concentrations were measured on a Varian Spectra AA at the University of Cape Town. Sulfur analyses performed prior to July 2008 were measured on a LECO 423 Sulfur Analyser and after July 2008 on a S632 Leco Sulfur Analyser housed at the University of Cape Town. Where iron, nickel and sulfur assays were available for all material obtained from microflotation tests, the pyrrhotite recovery was calculated. Pyrrhotite recovery was based on the assumption that all nickel was hosted in pentlandite, all copper in chalcopyrite. Therefore, once the amount of pentlandite and chalcopyrite were known, the amount of sulfur unaccounted for was assumed to be hosted by pyrrhotite and the proportion of pyrrhotite was accordingly calculated for Fe_7S_8 or Fe_9S_{10}. The method was unable to account for the proportion of solid solution nickel hosted by pyrrhotite or the presence of pyrite but within the limitations of this study, is the best possible method for calculating pyrrhotite recovery.